Journal of Mines, Metals and Fuels, *71(10): 1639-1644; 2023. DOI: 10.18311/jmmf/2023/35871*

Print ISSN : 0022-2755

Journal of Mines, Metals and Fuels

Contents available at: *www.informaticsjournals.com/index.php/jmmf*

Metallurgical Properties of CeLa Substituted Bio-Glass Ceramics

Priyam Mondal, Md. Ershad* and Ranjan Kumar

Department of Mechanical Engineering, Swami Vivekananda University, Barrackpore, Kolkata - 700121, India; priyamm@svu.ac.in, mdershad.rs.cer13@iitbhu.ac.in, ranjansinha.k@gmail.com

Abstract

To set up a bioglass of general structure given in Table 1. These five samples were ready in a crucible made up of alumina through a melting temperature of 1400±10 °C and normalized it. The glass powder pallet was made by the press and submerged in Simulated Body Liquid (SBF) in various time spans, and they're not entirely settled by FTIR examination. The morphology of the surface resolved to utilize a Checking by SEM. pH estimation of bioactive glass was done by pH meter and mechanical properties like Microhardness and Flexural strength were determined and found that it increases with increasing the concentration of REEs. The developed CeO_2 and La_2O_3 incorporated bioactive glasses were also found to enhance mechanical properties. Thus, the glasses with CeO_2 and La_2O_3 can be suitable candidates for bone implant application.

Keywords: *Flexural Strength, Microhardness, XRD, FTIR, CeO_2 and La_2O_3*

1.0 Introduction

Bioactive material ought to have a remarkable biochemical way of behaving like bone. The 45S5® bioactive has an excellent capacity to bond with both delicate and hard tissues. Hench chose to make a glass of the mol % creation 46.1 SiO_2-24.4 Na_2O-26.9 CaO-2.6 P_2O_5, known as 45S5 bioglass[1-5]. This sent off the field of bioactive pottery with numerous new materials and items[6,7]. Replacement of bioactive glasses with various progress and interesting earth metals like cerium, lanthanum, aluminum, and Silver to change their bioactive reaction has been concentrated on by various exploration bunches[8-12]. In this work, we concentrate on the impact of CeLa in vitro properties of the bioactive glass. Ce particles have been utilized in dental ceramic materials to impersonate normal teeth[13,14]. Cerium is additionally known to have bacteriostatic properties and has low harmfulness[15,16] in the base bioactive glass considering their clever outcome on osteoblastic cell duplication of different particles in the base bioactive glasses[17]. These bioactive glasses were lowered in SBF to support the headway of a bone-like apatite layer on their surfaces by using FTIR.

2.0 Materials and Methods

2.1 Composition and Glass Preparation

The wt% of CeO_2 to La_2O_3 content off the 45S5 glass has been specified in Table 1. Fine quartz was utilized to the wellspring of SiO_2. Insightful grades CaO, Na_2O, and P_2O_5 were separately utilized by melting. The necessary measures of scientific reagent grade CeO_2 and La_2O_3 were incorporated individually in the group given for the fractional replacement of SiO_2. The natural substances for various examples were appropriately gauged. Then the blending of various clumps was finished for 50 min in a pestle mortar. Bioactive material ought to have a remarkable biochemical way of behaving and biomechanical ability. The 45S5® bioactive has an

**Author for correspondence*

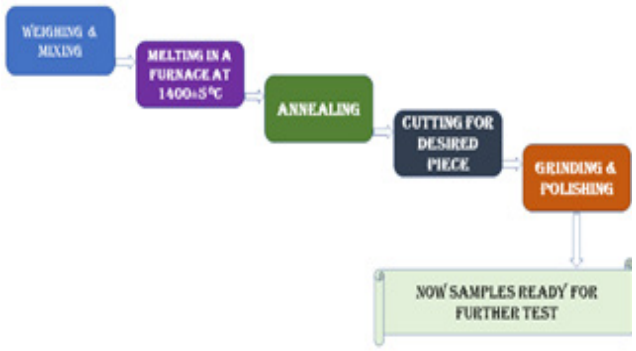

Figure 1. Flow chart of Bioglass samples prepared by the glass melting route.

Table 1. The compositions of bioactive glasses

Sample Id	Wt%					
	SiO_2	Na_2O	CaO	P_2O_5	CeO_2	La_2O_3
BG	45	24.5	24.5	6	0.0	0.0
Ce1	44.5	24.5	24.5	6	0.5	0.5
Ce2	44	24.5	24.5	6	1.0	1.0
La1	44.5	24.5	24.5	6	0.5	0.5
La2	44	24.5	24.5	6	1.0	1.0

excellent capacity to bond with both delicate and hard tissues. In this work, we concentrate on the impact of CeLa supplanting the thermo-mechanical, and in vitro properties of the bioactive glass. Ce particles have been utilized in dental materials to impersonate the fluorescence of normal teeth[13,14]. Cerium is additionally known to have bacteriostatic properties and has low harmfulness[15,16] in the base bioactive glass considering their clever outcome on osteoblastic cell duplication of different particles in the base bioactive glasses[17]. The ongoing work is stressed with the course of action and depiction of CeLa-modified glasses.

2.2 Preparation of Simulated Body Fluid (SBF)

The pre-arranged glass was drenched in SBF at 37.4°C at various spans differing from 1 to 13 days. The arrangement of SBF was ready as indicated by the reference given by Kokubo *et al.*,[14]. The pH was determined utilizing a digital pH meter after the submersion of tests for various spans.

Table 2. Ion content (mM/litre) of SBF and human blood plasma

Ion	Na^+	K^+	Ca^{2+}	Mg^{2+}	HCO_3^-	Cl^-	HPO_4^{2-}	SO_4^{2-}
Simulated Body Fluid	142	5	2.5	1.5	4.2	148	1	0.5
Blood plasma	142	5	2.5	1.5	27	103	1	0.5

2.3 X-ray Diffraction (XRD) of Powder Samples

The bioglass® tests were sliced and crushed to 150 microns and powder and further X-ray diffraction examination utilizing RIGAKU-Miniflex II (λ = 1.5405A) with a current of 35mA and tube voltage of 40 kV in a 2θ between 15-85°. The JCPDS was utilized as a source of references.

2.4 FTIR Absorbance Spectrometry for Structural Analysis

The designs of bioglass® tests were estimated at 24°C and the range of frequency 4000-400 cm^{-1} onward utilizing an FTIR (BT 27). The residue powder of the bioactive glass test was blended in with KBr in the proportion of 1:200 and the combinations were exposed to an evocable die at 12 bar load to create clear standardized discs. The pre-arranged plates were quickly exposed to an IR spectrophotometer to quantify the spectra to avoid moisture.

2.5 Density, Microhardness and Flexural Strength Measurements

The glass sample density was measured with (ASTM C20-00) involving distilled water a submersion fluid. The calculations were completed at 24°C. The weight of the glass was estimated by a digital balance (Wensar HPB 220) with a precision of ± 0.00001 g. The density (ρ) of the glass was evaluated by relation (1) as given below:

$$Density\ (\rho) = \frac{W_a}{W_a - W_b}\rho_b \qquad (1)$$

Where W_a & W_b are sample weights in air and water respectively, is the density of fluid.

For Microhardness, with accurately sized samples being surface finished after that hardness accomplished by a digital hardness analyzer, the size of the samples was 6mm x 6mm x 6mm as indicated by ASTM: C730-98. The indentation load range was going from 20 mN

and 3000 mN, at the speed of 2 mm/s, and was allowed to equilibrate for 16 seconds before test. Microhardness (H) was assessed utilizing equation (2),

$$Microhardness\ (H) = 1.854\frac{P}{d^2} \qquad (2)$$

Here P is the load applied to the samples and d (m) is the diagonal of the marks. The rectangular shape glass was ground and cleaned for 30×12×12 mm dimensions. Presently samples were prepared for the 3-point bending. The test was performed at 24 °C utilizing an Instron UTM (H10KL, Tinius Olsen, USA) with a crosshead speed of 0.5 mm/min and a full-scale 10kN load. Flexural strength (σ) was assessed by ASTM C1674-11 as (3),

$$Flexural\ Strength(\sigma) = \frac{3PL}{2bh^2} \qquad (3)$$

Where *P* is the applied load for the specimen to break, *L*, *b*, and *h* are the span length, breadth, and height of the specimen correspondingly.

3.0 Results and Discussion

3.1 X-Ray Analysis of Samples

X-RD is flexible, NDT that uncovers thorough data about substance creation and crystallographic nature, and in glass ceramics designs, huge peaks are found, which is why all given bioglass® tests are crystalline[18]. It shows that all the SiO_2-Na_2O-CaO-P_2O_5 and CeLa doped glass tests have been melted appropriately and changed over into glassy ceramics in Figure 2.

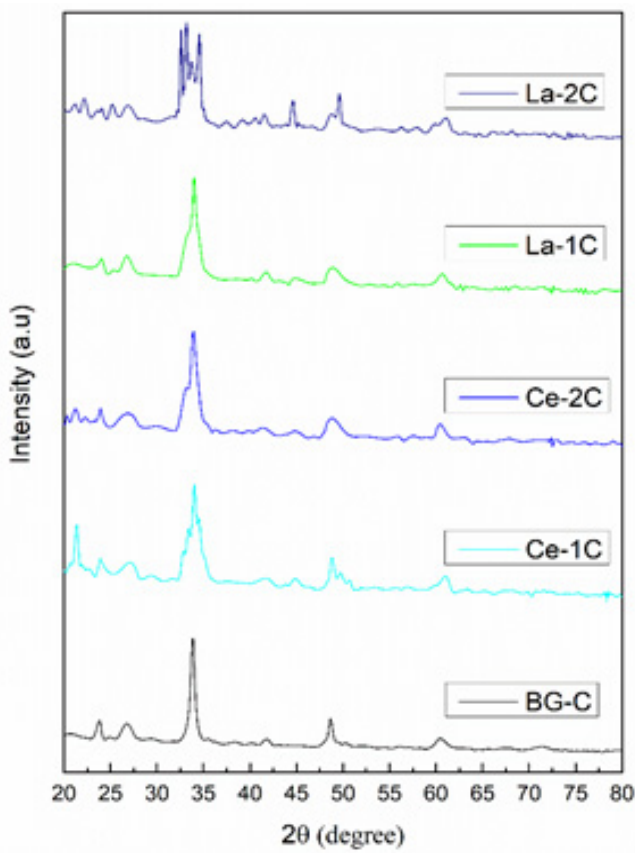

Figure 2. XRD patterns of the bioactive glass-ceramic samples after soaking them in the SBF solution for 21 days.

3.2 FTIR Assessment

Absorbance spectra bands in the glass samples after dipping in SBF for various time spans 1, 4, 8, 13, and 19 days. Figure 3 shows the infrared spectral groups of up to La-2C samples when its submersion in SBF for 13 days. The new groups were found to show up following 13-day drenching in SBF at around 802cm^{-1} which compares to Si-O-Si bend. The groups relating to the frequencies of 1379 and 1628 cm^{-1} are related to C-O (carbonate) stretching and a significant peak at around 3093cm^{-1} can be relegated because of the presence of O-H (Hydroxyl) bunches on the outer layer of the samples. The vibrational groups at around 918cm^{-1} are made because of PO_4 (P-O extending) in Figure 3. All examples are displayed in comparable trademark groups. The vibrational groups

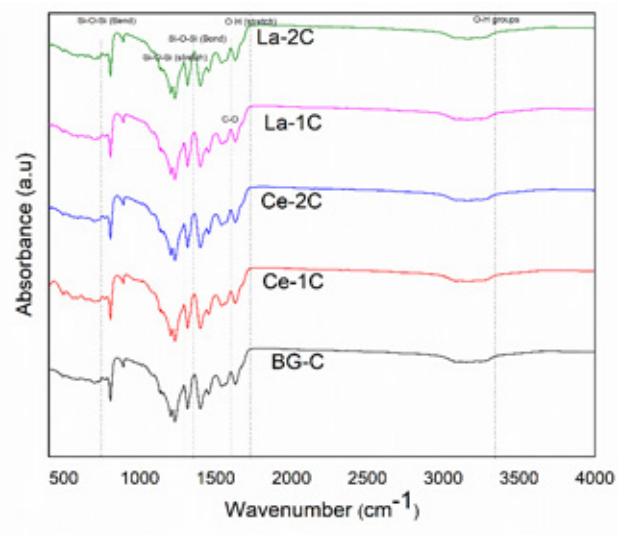

Figure 3. FTIR absorption spectra of all bioglass samples after soaking them in SBF for 19 days.

at around 655 cm^{-1} are because of the Si-O-Si bowing vibrational bending mode so might be because of the formation of SiO_6 octahedra in the SBF-treated example. The delayed time of treatment of the example in SBF shows a comparative way of behaving well because of the development of the Hydroxyl Carbonate Apatite (HCA).

3.3 Density, Flexural Strength and Microhardness

Figure 4 shows the density of the glasses as an element of CeO_2/La_2O_3 with error bars. Obviously, an increase in the proportion of REEs with increasing CeO_2 replacement brought about an enhancement in the density of glasses from 2.69 to 2.72 g/cc accordingly. This is ascribed because of the explanation that the cerium particles could have involved interstitial destinations inside the glass network[19,20]. Subsequently, it expanded the densities and brought about making new bonds with the fuse of lanthanum particles in the bioactive glasses. It has caused support for the glass structure and brought about improve compression of the glass samples.

Figure 4, shows the density of the glass ready from the melting root. The Density of Cerium and Lanthanum subbed glass (0.5-1.0 wt%) glasses were estimated by Archimedes' principle and viewed as 2.781, 2.799, 2.811, and 2.834 gm/cm^3 separately. Cerium and Lanthanum trade for silicon might have been found to increment in thickness because of the consequence of the substitution of lighter atoms (Si - 2.65 gm/cm^3) by heavier ones (Ce - 6.76 gm/cm^3) and (La - 6.15 gm/cm^3. Then again, because of the smaller size of La particles (ionic radius ~1.061 Å) and Ce particles (ionic radius ~1.034 Å) particles, it very well may be embraced a comparable structure and as a replace for the Ce^{4+}/La^{3+} particles, it very well may be lead to expand the thickness of the glass[21]. The mechanical examination aftereffect of base glass Figure 5, displays microhardness and flexural strength of 8.4 GPa and 69.12 MPa separately while the microhardness and flexural strength of subbed bioglass* shows an increase in microhardness (Ce 1C, Ce-2C, La-1C, and La-2C are 6.98, 7.1, 8.2 and 8.3 GPa) and flexural strength (51.2, 57.11, 64.12 and 69.22 MPa) with expanding substituent focus. In this manner, because of the conservativeness of the glass structure, the microhardness and flexural strength were enhanced by replacing the REEs particles.

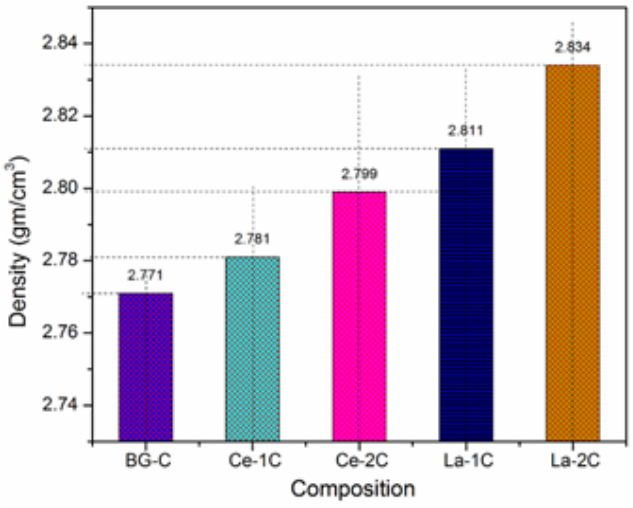

Figure 4. Density of substituted bioglass samples.

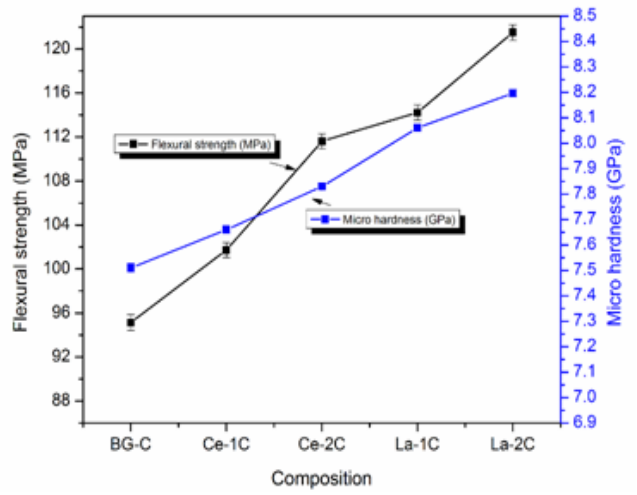

Figure 5. Flexural strength and Microhardness of substituted bioglass samples.

4.0 Conclusion

A similar study was made on, the physic-mechanical and in vitro bioactivity of 45S5 bioactive glasses subbed with differing centralizations of La_2O_3 and CeO_2 with SiO_2. It was seen that microhardness and flexural strength increments with expanding grouping of La_2O_3 and CeO_2 while nucleation and crystallization temperature diminish. The accompanying ends were drawn from these examinations: The flexural strength, as well as Microhardness of the subbed test, has been expanded by expanding the convergence of oxides. Notwithstanding Ce^{4+} and La^{3+} particles were tracked down that

mechanobiological properties enhance with the change in the content of these REEs. XRD example of altered 45S5 glass shows crystalline phase presence of Ce^{4+} and La^{3+} particles after heat treatment. In FTIR spectra, the Hydroxy Carbonate Apatite (HCA) layer is available after the SBF treatment.

5.0 Acknowledgment

The corresponding authors gratefully acknowledge the Director, IIT (BHU) Varanasi-221005, India, and the Department of Mechanical Engineering, Swami Vivekananda University, Kolkata-700126, India for providing necessary facilities for the present research work.

6.0 References

1. Hench LL. Bio-ceramics. J Am Ceram Soc. 1998;74(7):1487-510. https://doi.org/10.1111/j.1151-2916.1991.tb07132.xt
2. Gerhardt LC, Boccaccini AR. Bioactive Glass and Glass-Ceramic Scaffolds for Bone Tissue Engineering. Materials. 2010; 3:3867-910. https://doi.org/10.3390/ma3073867 PMid:28883315 PMCid:PMC5445790t
3. Ylanen HO. Bioactive glasses materials properties and applications. Woodhead Publishing Limited. Biomaterials. 2011; 6:1-288.t
4. Heness G, Ben-Nissan B. Innovative bio-ceramics. Mater Forum. 2004; 27:104-14. https://doi.org/10.1142/9789812702692_0024t
5. Ershad M, Vyas VK, Prasad S, Ali A, Pyare R. Effect of Sm_2O_3 substitution on mechanical and biological properties of 45S5 bioactive glass. J Aust Ceram Soc. 2018; 54(4):621-30. https://doi.org/10.1007/s41779-018-0190-7t
6. Fredholm YC, Karpukhina N, Law RV, Hill RG. Strontium-containing bioactive glasses: Glass structure and physical properties. J Non-Cryst Solids. 2010; 356:2546-51. https://doi.org/10.1016/j.jnoncrysol.2010.06.078t
7. Balamurugan A, Rebelo AH, Lemos AF, Rocha JH, Ventura JM, Ferreira JM. Suitability evaluation of sol–gel derived Si-substituted hydroxyapatite for dental and maxillofacial applications through *in vitro* osteoblasts response. Dent Mater. 2008; 24:1374-80. https://doi.org/10.1016/j.dental.2008.02.017 PMid:18417203t
8. Oki A, Parveen B, Hossain S, Adeniji S, Donahue H. Preparation and in vitro bioactivity of zinc containing sol-gel–derived bioglass materials. J Biomed Mater Res A. 2004; 69:216-21. https://doi.org/10.1002/jbm.a.20070 PMid:15057994t
9. Saboori A, Sheikhi M, Moztarzadeh F, Rabiee M, Hesaraki S, Tahriri M. Sol–gel preparation, characterisation and in vitro bioactivity of Mg containing bioactive glass. Adv Appl Ceram. 2009; 108:155-61. https://doi.org/10.1179/174367608X324054t
10. Du W, Kuraoka K, Akai T, Yazawa T. Study of Al_2O_3 effect on structural change and phase separation in Na_2O-B_2O_3-SiO_2 glass by NMR. J Mater Sci. 2000; 35:4865-71. https://doi.org/10.1023/A:1004845817600 t
11. Yun YH, Bray PJ. Nuclear magnetic resonance studies of the glasses in the system Na_2O-B_2O_3-SiO_2. J Non Cryst Solids. 1978. Available from: https://linkinghub.elsevier.com/retrieve/pii/0022309378900200. https://doi.org/10.1016/0022-3093(78)90020-0t
12. Dell WJ, Bray PJ, Xiao SZ. 11B NMR studies and structural modeling of Na_2O-B_2O_3-SiO_2 glasses of high soda content. J Non Cryst Solids. 1983. Available from: https://linkinghub.elsevier.com/retrieve/pii/0022309383900972. https://doi.org/10.1016/0022-3093(83)90097-2t
13. Manara D, Grandjean A, Neuville DR. Structure of borosilicate glasses and melts: A revision of the Yun, Bray, and Dell model. J Non Cryst Solids. 2009. Available from: https://linkinghub.elsevier.com/retrieve/pii/S0022309309005845. https://doi.org/10.1016/j.jnoncrysol.2009.08.033t
14. Kokubo T, Takadama H. How useful is SBF in predicting in vivo bone bioactivity. Biomaterials. 2006; 27:2907-15. https://doi.org/10.1016/j.biomaterials.2006.01.017 PMid:16448693t
15. Ali A, Singh BN, Yadav S, Ershad M, Singh SK, Mallick SP, Pyare R. CuO assisted borate 1393B3 glass scaffold with enhanced mechanical performance and cytocompatibility: An *In vitro* study. J Mech Behav Biomed Mater. 2021; 114:104231. https://doi.org/10.1016/j.jmbbm.2020.104231 PMid:33276214t
16. Ershad M, Vyas VK, Prasad S, Ali A, Pyare R. Synthesis and characterization of cerium- and lanthanum-containing bioactive glass. Key Eng Mater. 2017; 751:617-28. https://doi.org/10.4028/www.scientific.net/KEM.751.617t
17. Nayak JP, Kumar S, Bera J. Sol-gel synthesis of bio-glass-ceramics using rice husk ash as a source for silica and its characterization. J Non-Cryst Solids. 2010; 356:1447-51. https://doi.org/10.1016/j.jnoncrysol.2010.04.041t

18. Vyas VK, Kumar AS, Ali A, Prasad S, Srivastava P, Mallick SP, Ershad M, Singh SP, Pyare R. Assessment of nickel oxide-substituted bioactive glass-ceramic on *in vitro* bioactivity and mechanical properties. Bol Soc Esp Ceram Vidrio. 2016; 55(6):228-38. https://doi.org/10.1016/j.bsecv.2016.09.005t
19. Ershad M, Ali A, Mehta NS, Singh RK, Singh SK, Pyare R. Mechanical and biological response of ($CeO^{2+}La_2O_3$)-substituted 45S5 bioactive glasses for biomedical application. J Aust Ceram Soc. 2020; 56(4):1243-52. https://doi.org/10.1007/s41779-020-00471-3t
20. Ali A, Ershad M, Hira S, Pyare R. Mechanochemical and in vitro cytocompatibility evaluation of zirconia-modified silver-substituted 1393 bioactive glasses. Bol Soc Esp Ceram Vidrio. 2022; 61(1):64-75. https://doi.org/10.1016/j.bsecv.2020.07.002